

## Peptide–Antibody Complex as Handle for Single-Molecule Cut &amp; Paste

Mathias Strackharn,<sup>[a]</sup> Stefan W. Stahl,<sup>[b]</sup> Philip M. D. Severin,<sup>[a]</sup> Thomas Nicolau,<sup>[a]</sup> and Hermann E. Gaub<sup>\*[a]</sup>

Feynman is frequently quoted for having foreseen that individual atoms may be arranged one-by-one to form functional assemblies.<sup>[1]</sup> The seminal work by Don Eigler and colleagues<sup>[2,3]</sup> convincingly proved the validity of these concepts: functional assemblies of atoms forming quantum corrals showed emergent novel properties. In the life sciences, Hans Kuhn realized rather early that for many multistep biological reactions, not only the sequence but also the arrangement of the individual enzymes plays a crucial role. He envisaged that in order to investigate their interaction, novel approaches would be needed: he wished to have "...molecular pliers to pick and place individual enzymes to create functional assemblies with designed properties."<sup>[4]</sup> The application of bottom-up strategies to assemble biomolecular complexes, however, turned out to be rather challenging. A quite vivid dispute was fought in a series of papers between Smalley and Drexler on where these difficulties arise from and whether fundamental limitations prevent a molecule for molecule assembly of biomolecules in electrolyte ambient and at physiologic temperatures.<sup>[5]</sup> With the development of single-molecule cut-and-paste (SMC&P) we overcame these difficulties and provided a platform technology for the assembly of biomolecules at surfaces.<sup>[6]</sup> It combines the Å-positioning precision of atomic force microscopy (AFM)<sup>[7,8]</sup> with the selectivity of DNA hybridization to pick individual molecules from a depot chip and to arrange them on a target site by pasting the molecules one-by-one.<sup>[9]</sup> The advanced methods of single-molecule fluorescence detection<sup>[10–14]</sup> allowed us to localize the pasted molecules with nanometer accuracy and to show that the deposition accuracy is presently only limited by the length of the spacers used to couple the DNA handles and anchors to tip and construction site, respectively.<sup>[15]</sup>

In the various SMC&P implementations realized to date, the system of hierarchical binding forces was built from DNA duplexes of suitable geometry and sequence. Since one of the major goals, which spurs the development of the SMC&P technology, is the ability to arrange proteins, for example, in enzymatic networks of predefined composition and proximity, mo-

lecular anchors and handles should ultimately be of such a kind that they can be co-expressed with the proteins, for example, as tags on a protein chip. As a first step in this direction, we chose in this Communication a peptide–antibody complex to replace the DNA-based handle complex in the conventional SMC&P design. This single-chain antibody, which is part of a larger family, was selected by the Plückthun group to recognize a 12 aa long segment of a polypeptide chain with picomolar affinity.<sup>[16]</sup> In previous studies we had investigated by single-molecule force spectroscopy and molecular dynamics (MD) simulations several different peptides and antibodies and investigated the influence of the attachment site on the unbinding mechanisms.<sup>[17,18]</sup> We could confirm that the antibody (when covalently attached at the C-terminal end) stays intact when the peptide is pulled out of the binding pocket. Herein, we used this antibody immobilized at the AFM cantilever tip to pick up a fluorescently labeled transfer DNA–peptide chimera via its peptide tag and paste it on the target site of the chip.

Using a microspotter, we deposited microdroplets of a DNA solution onto a pretreated glass surface resulting in approximately 50 µm-sized spots with a distance of 70 µm (see Supporting Information, Figure 1). The ssDNA was allowed to covalently bind to the surface via PEG spacers. One drop contained ssDNA with a reactive 5' end. The resulting spot later on forms the depot. The other drop contained DNA with a reactive 3' end and the resulting spot forms the target. The depot area was then loaded with a complementary ssDNA strand, which was extended at the 3' end by a 13-amino-acid-long handle peptide and labeled at the 5' end with an atto647N fluorophore. For simplicity, this construct is called transfer strand. Single-chain antibodies were covalently attached via PEG spacers to the AFM cantilever tip (see Figure 1a for a cartoon of the SMC&P process).

To pick up an individual DNA strand, the AFM tip was lowered at the depot area, allowing the antibody at the tip to bind to the peptide at the end of the DNA strand to be transferred. Upon retract, typically the force gradually increased and finally dropped as shown in Figure 1b, where the force is plotted as a function of the distance. We chose the functionalization density of the tip and the surface such that typically only in every second attempt we found this characteristic force curve, indicating that exactly one DNA strand was picked up. In the majority of the other 50% of the attempts we found no measurable force upon retract, indicating that no molecule was picked up. In these cases, we repeated the pick-up cycle. Only in very rare cases (<2%) did we find higher values for the unbinding force, indicating that more than one molecule was picked up.

[a] M. Strackharn, P. M. D. Severin, T. Nicolau, Prof. Dr. H. E. Gaub  
Center for Nanoscience and Department of Physics  
University of Munich, Amalienstrasse 54  
80799 München (Germany)  
Fax: (+49) 89-2180-2050  
E-mail: gaub@lmu.de

[b] S. W. Stahl  
Center for Integrated Protein Science (CIPSM)  
Center for Nanoscience and Department of Physics  
University of Munich, Amalienstrasse 54  
80799 München (Germany)

Supporting information for this article is available on the WWW under <http://dx.doi.org/10.1002/cphc.201100765>.

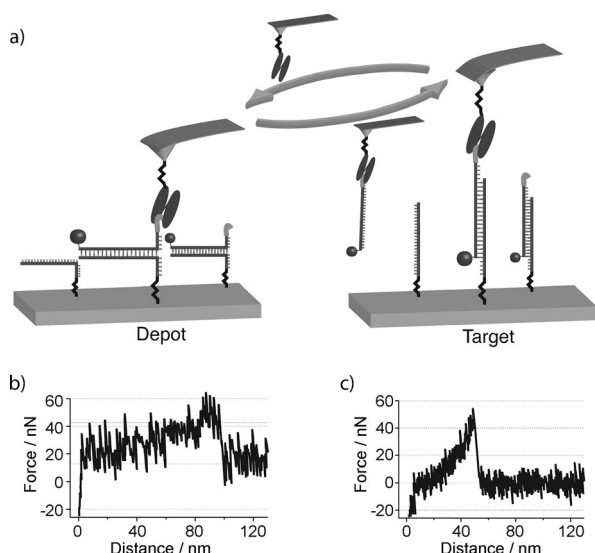


**Figure 1.** a) Schematic representation of a typical SMC&P cycle. A single-chain antibody fragment is covalently bound to the cantilever tip. When lowered to the depot area surface, the antibody binds to a peptide at the end of a DNA strand, which is attached to the surface via 40 bp in zipper mode. When the tip is pulled back, the basepairs open up one by one. The transfer construct remains attached to the cantilever and may be transferred to the target area. Here, the cantilever is lowered again such that the DNA part of the construct binds to the DNA target anchor. When the cantilever is retracted, this time the DNA bases are loaded in shear geometry and the antibody-peptide bond yields. The transfer construct remains in the target area and the cantilever can be used for the next transfer cycle again. b,c) Force-distance graphs of typical rupture events in the depot (b) and target (c) areas.

The AFM tip was now moved to a chosen position in the target area and gradually lowered, allowing the transfer strand to hybridize to the target DNA. Upon retract again, the force-versus-distance curve was recorded. A typical example is given in Figure 1c. As can be seen, the force peaks at a much higher value, typically at 40 pN. Since this value is much lower than the force required to break the DNA shear bond, we conclude with a high certainty that the transfer DNA was deposited in the target area. Details of the probabilities for the rupture of bonds in series are given elsewhere.<sup>[19]</sup>

To corroborate that the force required to unzip the anchor duplex is lower than the binding force of the peptide-antibody complex and that the latter is lower than the force required to unbind the DNA duplex in shear geometry we investigated the bond strength of the three complexes in a separate series of experiments. Since unbinding forces depend in a first-order approximation given by the Bell-Evans model on the logarithm of the force loading rate,<sup>[20]</sup> we varied the latter by one and a half orders of magnitude. The result is depicted in Figure 2. For the lowest curve, the unbinding force of the depot-transfer duplex was measured under conditions where both were covalently attached to tip and sample surface via PEG spacers. Note that the depot strand was attached at its 5' end and the transfer strand was attached at the 3' end, mimicking the geometry during pickup. For the red curve, the peptide was attached to the sample surface, allowing the antibody,

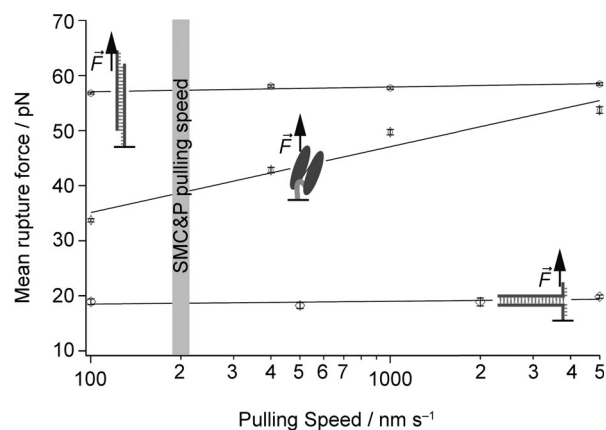


**Figure 2.** Dependency of the mean rupture force on the pulling speed. The mean rupture force for opening the 40 bp DNA in shear geometry is nearly 60 pN. The mean rupture force of the peptide-antibody complex is significantly lower than that of the DNA in shear geometry and shows a logarithmic dependence on the loading rate. The 40 bp DNA in unzip geometry opens at a mean rupture force of around 20 pN. Error bars depict fitting errors from fitting the force distributions. Highlighted is the pulling speed chosen for the deposition process.

which was covalently attached to the tip, to bind the peptide in exactly the same geometry as during pick up. As can be seen, both lines differ drastically in their slopes, but more important for the issues discussed here, the force required to unzip the two DNA strands is significantly lower than that required to break the peptide-antibody bond for the entire range of pulling speeds. Since the curve of the antibody-peptide complex lies significantly below the curve recorded for the DNA duplex in shear geometry (note that the target strand was now attached with the 3' end to the surface), it is predominantly the peptide-antibody complex that ruptures in the deposition process. From this graph we chose the optimum pulling speed window around 200 nm sec<sup>-1</sup> for the SMC&P experiments described below.

In parallel to the SMC&P experiments, we followed the deposition process of the individual molecules microscopically in total internal fluorescence excitation. Details of the device are given elsewhere,<sup>[21]</sup> but it is important to note that the custom-built combined AFM-TIRF microscope was optimized for vibrational stability, which is essential to avoid the coupling of mechanical noise into the AFM via the immersion fluid required for high NA optical microscopy. Figure 3a shows a micrograph taken at the beginning of the deposition process in the target region. In Figure 3b the left image shows the scattered light from the tip and the emission of the fluorophore. The second image depicts the same spot after the tip has left the evanescent zone, leaving only the deposited fluorophore visible (a movie of this process is provided in the Supporting Information). With standard techniques, the position of this fluorophore was then determined with an accuracy of 1.4 nm.

After the deposition of the transfer strand in the target area, the tip is again in its original state and therefore ready to pick up another transfer strand from the storage area. Since the antibody-peptide bond is reversible, this pick-up and deposit

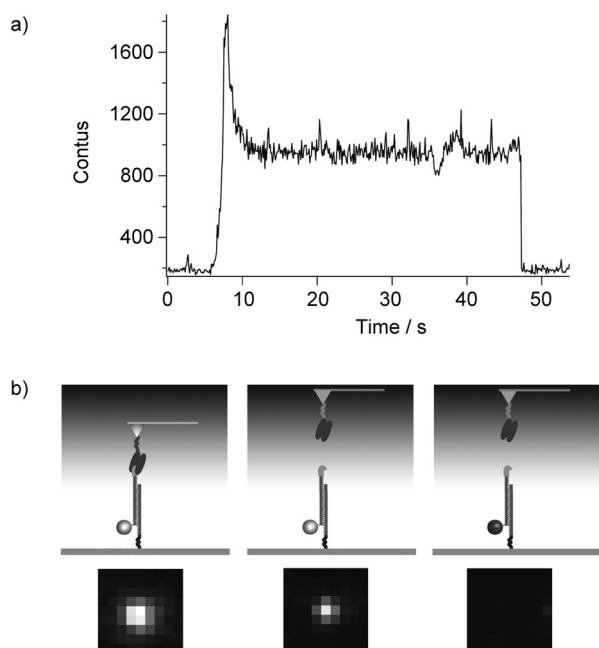


**Figure 3.** Deposition of a single DNA-peptide construct. The loaded cantilever is lowered towards the target area, where the DNA-peptide construct is deposited, when the lever is withdrawn. a) Fluorescence timetrace and b) cartoon of the process. When the cantilever enters the evanescent field of the TIR illumination, fluorescence from the dye-labeled construct and scattered light from the cantilever tip contribute to the signal, whereas after retraction of the cantilever, only fluorescence of the dye molecule is measured. No signal is measured after photobleaching of the dye.

or—in other words—molecular cut-and-paste process may be carried out for many cycles, allowing one molecule after the other to be transferred, unless damage to the antibody occurs during the forced unbinding of the antibody-peptide complex. To demonstrate that the antibody-peptide complex is robust and very well suited as handle complex at the AFM tip, we as-

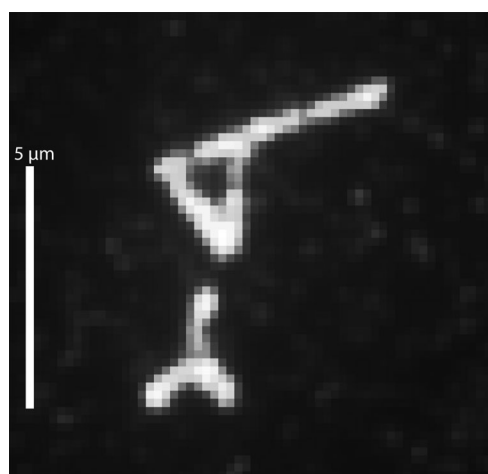


**Figure 4.** The robustness of the SMC&P process is demonstrated by the molecule-by-molecule assembly of a microscopic pattern showing a cantilever and an antibody. The pattern is assembled from approximately 600 molecules.

sembled the molecular pattern depicted in Figure 4 from approximately 600 transfer strands in a molecule-by-molecule copy-and-paste process. This convincingly demonstrates that the hierarchical force system, which is a prerequisite for SMC&P, may well be realized based on peptides or protein modules for anchor and/or handle groups. One may as well envisage covalent or organometallic coupling schemes<sup>[22,23]</sup> or even external modulation of the interaction forces by externally controlled Coulomb interactions<sup>[24]</sup> to expand the toolbox for single-molecule assembly.

## Experimental Section

All measurements described in the manuscript were carried out with a custom-designed combined AFM/TIRF microscope described in detail elsewhere.<sup>[21]</sup> We provide a detailed description of AFM measurements, TIRF microscopy, single-chain antibody fragment preparation, peptide synthesis, surface preparation, microstructuring with a microplotter, and oligomer sequences in the Supporting Information.

## Acknowledgements

This work was supported by the Volkswagen foundation, the Nano Initiative Munich and the German Science Foundation (SFB 863).

**Keywords:** biophysics • nanostructures • scanning probe microscopy • single-molecule studies • TIRF microscopy

- [1] R. P. Feynman, *Eng Sci* **1960**, *23*, 22–36.
- [2] M. F. Crommie, C. P. Lutz, D. M. Eigler, *Science* **1993**, *262*, 218–20.
- [3] T. A. Jung, R. R. Schlittler, J. K. Gimzewski, H. Tang, C. Joachim, *Science* **1996**, *271*, 181–184.
- [4] H. Kuhn, *Verhandlungen der Schweizerischen Naturforschenden Gesellschaft* **1965**, 245–266.
- [5] R. Baum, *Chem. Eng. News* **2003**, *81*, 37–42.
- [6] S. K. Kufer, E. M. Puchner, H. Gump, T. Liedl, H. E. Gaub, *Science* **2008**, *319*, 594–6.
- [7] G. Binnig, C. F. Quate, C. Gerber, *Phys. Rev. Lett.* **1986**, *56*, 930–933.
- [8] B. Drake, C. B. Prater, A. L. Weisenhorn, S. A. C. Gould, T. R. Albrecht, C. F. Quate, D. S. Cannell, H. G. Hansma, P. K. Hansma, *Science* **1989**, *243*, 1586–1589.
- [9] E. M. Puchner, S. K. Kufer, M. Strackharn, S. W. Stahl, H. E. Gaub, *Nano Lett.* **2008**, *8*, 3692–5.
- [10] W. E. Moerner, L. Kador, *Phys. Rev. Lett.* **1989**, *62*, 2535–2538.
- [11] T. Schmidt, G. J. Schutz, W. Baumgartner, H. J. Gruber, H. Schindler, *Proc. Natl. Acad. Sci. USA* **1996**, *93*, 2926–9.
- [12] R. D. Vale, T. Funatsu, D. W. Pierce, L. Romberg, Y. Harada, T. Yanagida, *Nature* **1996**, *380*, 451–3.
- [13] A. Zurner, J. Kirstein, M. Dobliger, C. Bräuchle, T. Bein, *Nature* **2007**, *450*, 705–8.
- [14] G. Seisenberger, M. U. Ried, T. Endress, H. Buning, M. Hallek, C. Bräuchle, *Science* **2001**, *294*, 1929–32.
- [15] S. K. Kufer, M. Strackharn, S. W. Stahl, H. Gump, E. M. Puchner, H. E. Gaub, *Nat Nanotechnol* **2009**, *4*, 45–9.
- [16] C. Zahnd, S. Spinelli, B. Luginbuhl, P. Amstutz, C. Cambillau, A. Pluckthun, *J Biol Chem.* **2004**, *279*, 18870–7.
- [17] J. Morfill, J. Neumann, K. Blank, U. Steinbach, E. M. Puchner, K. E. Gottschalk, H. E. Gaub, *J. Mol. Biol.* **2008**, *381*, 1253–66.
- [18] J. Morfill, K. Blank, C. Zahnd, B. Luginbuhl, F. Kuhner, K. E. Gottschalk, A. Pluckthun, H. E. Gaub, *Biophys. J.* **2007**, *93*, 3583–90.
- [19] G. Neuert, C. H. Albrecht, H. E. Gaub, *Biophys. J.* **2007**, *93*, 1215–23.

- [20] F. Kühner, H. E. Gaub, *Polymer* **2006**, *47*, 2555–2563.
- [21] H. Gump, S. W. Stahl, M. Strackharn, E. M. Puchner, H. E. Gaub, *Rev. Sci. Instrum.* **2009**, *80*, 063704.
- [22] B. M. Gaub, C. Kaul, J. L. Zimmermann, T. Carell, H. E. Gaub, *Nanotechnology* **2009**, *20*, 434002.
- [23] P. Knochel, S. Z. Zimdars, S. X. M. du Jourdin, F. Crestey, T. Carell, *Org. Lett.* **2011**, *13*, 792–795.
- [24] M. Erdmann, R. David, A. R. Fornof, H. E. Gaub, *Nat. Chem.* **2010**, *2*, 745–9.

---

Received: September 29, 2011

Published online on December 19, 2011

---

# CHEMPHYSICHEM

## Supporting Information

© Copyright Wiley-VCH Verlag GmbH & Co. KGaA, 69451 Weinheim, 2012

### **Peptide–Antibody Complex as Handle for Single-Molecule Cut & Paste**

Mathias Strackharn,<sup>[a]</sup> Stefan W. Stahl,<sup>[b]</sup> Philip M. D. Severin,<sup>[a]</sup> Thomas Nicolaus,<sup>[a]</sup> and Hermann E. Gaub<sup>\*[a]</sup>

cphc\_201100765\_sm\_miscellaneous\_information.pdf

cphc\_201100765\_sm\_2.avi

# Supplementary Information

## Peptide:Antibody Complex as Handle for Single-Molecule Cut & Paste

Mathias Strackharn<sup>1,\*</sup>, Stefan W. Stahl<sup>1,2</sup>, Philip M. D. Severin<sup>1</sup> Thomas Nicolaus<sup>1</sup>,  
and Hermann E. Gaub<sup>1</sup>

<sup>1</sup> Center for Nanoscience and Department of Physics, University of Munich, Amalienstraße 54,  
80799 Munich, Germany

<sup>2</sup> Center for Integrated Protein Science (CIPSM), Munich, Germany

\* [mathias.strackharn@physik.uni-muenchen.de](mailto:mathias.strackharn@physik.uni-muenchen.de)

All measurements described in the manuscript were carried out with a custom designed combined AFM/TIRF microscope described in detail in <sup>[21]</sup>. Here we provide the description of those parts and procedures, which are relevant to the experiments described in the main text:

### AFM measurements

The spring constants of the DNA modified cantilevers were calibrated in solution using the equipartition theorem <sup>[25]</sup>, <sup>[26]</sup>. For the single-molecule force spectroscopy BL-AC40TS-C2 levers (Olympus, Tokyo, Japan) and for SMC&P experiments MLCT-AUHW levers (Bruker, Camarillo, USA) were used. The protocol for the functional assembly as well as the data recording was programmed using Igor Pro (Wave Metrics, Lake Oswego, USA) and an Asylum Research MFP3D controller (Asylum Research, Santa Barbara, USA), which provides ACD and DAC channels as well as a DSP board for setting up feedback loops. Cantilever positioning for pick-up and delivery was controlled in closed-loop operation. The typical cycle time for one functional assembly process lies between 2 and 3 seconds depending on the sample orientation and the

traveling distance between depot and target area. The positioning feedback accuracy is  $\pm 3$  nm however long term deviations may arise due to thermal drift. Extension velocities are set to  $2 \mu\text{m/s}$  in the depot area and  $200 \text{ nm/s}$  in the target area. Force spectroscopy data was converted into force-extension curves and the most probable rupture force was obtained using the program IGOR Pro 6.22 (Wave Metrics, Lake Oswego, USA) and a set of custom-made procedures. Rupture forces for each retraction speed were plotted in histograms and fitted with Gaussians to determine the most probable rupture forces.

### **TIRF microscopy**

The fluorescence microscopy measurements were carried out with objective-type TIRF excitation on a microscope that was especially designed for a stable combination of AFM with TIRFM<sup>[21]</sup>. We excited with a fiber-coupled 637 nm diode laser (iBeam smart, TOPTICA, München, Germany) through a 100x/1.49 oil immersion objective lens (Nikon CFI Apochromat TIRF, Japan). As excitation filter, beam splitter, and emission filter a BrightLine HC 615/45, a Raman RazorEdge 633 RS, and a Chroma ET 685/70 (AHF, Tübingen, Germany) were used respectively. Images were taken with a back-illuminated EMCCD camera (DU-860D, Andor, Belfast, Ireland). Fluorescence image sequences were taken at 10 Hz frame rate, gain 150, 1 MHz readout rate in frame transfer mode. The camera was operated at  $-75 \text{ }^\circ\text{C}$ .

### **Preparation of the C11L34 single chain antibody fragment**

The C11L34 single chain antibody fragment was prepared as described in<sup>[18]</sup>. The scFv construct harbored a C-terminal His tag followed by a Cys to allow for site-specific immobilization and was obtained by periplasmic expression in *E. coli* SB536. C11L34 was purified by  $\text{Ni}^{2+}$  and immobilized antigen affinity chromatography according to standard protocols. The concentration was adjusted to  $2.5 \text{ mg/ml}$  in storage buffer containing  $50 \text{ mM}$  sodium phosphate,  $\text{pH } 7.2$ ,  $50 \text{ mM}$  NaCl and  $10 \text{ mM}$  EDTA.

### **Preparation of GCN4 peptides**

GCN4 peptides with the sequence CYHLENEVARLKK were synthesized manually in syringe reaction chambers. 0.05 g Wang resin (Iris, Marktredwitz, Germany) were incubated with 10 eq (of the maximal loading capacity of the resin) Fmoc-L-Lys(Boc)-OH (Iris, Marktredwitz, Germany) for 4 h. The incubation was repeated for another 4 h. For the measurement of the resin loading 500  $\mu$ l of DMF (Sigma, Taufkirchen, Germany) with 20 % Piperidine (Fluka, St. Gallen, Switzerland) were added to 3 mg of the resin. The solution was shaken for 1 h, the 3 ml DMF were added. By measuring the extinction at 300 nm of a 1:10 dilution with DMF with 20% Piperidine the resin loading was determined. Remaining hydroxyl groups on the Wang resin were blocked by esterification with acetic anhydride. All other Fmoc-protected amino acids (Iris, Marktredwitz, Germany) were added by applying the following procedure: 10 eq amino acid and 100 eq HOBT (Fluka, St. Gallen, Switzerland) were dissolved in DMF, 10 eq DIC (Fluka, St. Gallen, Switzerland) was added and the solution was shaken for 1 h. Then 10 eq DIPEA (Fluka, St. Gallen, Switzerland) were added and solution was shaken for 1h again. The process was once repeated. Then then the resin was washed with 10 ml DMF, 10 ml DCM, 10 ml Ether and 6 ml DMF, again. Fmoc protection groups were removed by incubating the resin in DMF with 20 % Piperidine for 20 min twice. The resin was then flushed with 10 ml DMF, 10 ml DCM (Carl Roth, Karlsruhe, Germany), 10 ml Ether (Sigma, Taufkirchen, Germany) and 6 ml DMF. The peptide was finally separated from the resin by 3 h shaking in 50  $\mu$ l p-Thiocresol (Fluka, St. Gallen, Switzerland), 50  $\mu$ l Thioanisol (Fluka, St. Gallen, Switzerland) and 300  $\mu$ l TFA (Sigma, Taufkirchen, Germany). The solution was transferred into a centrifuge tube, where the peptide was precipitated with 10 ml Ether at -80 °C. The solution was centrifuged at 4 °C and 4600 g and the pellet was washed in Ether six times. Finally the pellet was resolved in a 3:1 ddH<sub>2</sub>O/tertButanol (Sigma, Taufkirchen, Germany) solution and lyophilized.

### **Preparation of cantilevers**

Cantilevers (MLCT, Bruker, Camarillo, USA) were always oxidized in a UV-ozone Cleaner (UVOH 150 LAB, FHR Anlagenbau GmbH, Ottendorf-Okrilla, Germany). For single molecule force spectroscopy experiments and single molecule deposition they were silanized with 3-aminopropyltrimethoxysilane (ABCR, Karlsruhe, Germany), baked at 80 °C, pre-incubated with sodium borate buffer (pH 8.5), PEGylated with NHS-PEG-Maleimide (MW 5000, Rapp Polymere, Tübingen, Germany), and washed with ddH<sub>2</sub>O. According to the experiment type either C11L34 antibodies at a concentration of 2.5 mg/ml or reduced thiolated transfer DNA at a concentration of 10 μM was bound to the pegylated cantilevers at 8 °C for 2 h. Cantilevers were then washed with PBS buffer. In case of the SMC&P experiment, where molecules were assembled to the pattern of a cantilever with antibody at the tip, the cantilever was silanized with (3-Glycidoxypropyl)trimethoxysilane (ABCR, Karlsruhe, Germany), baked at 80 °C for 30 min and incubated overnight at 8 °C with 1mg/ml aminodextrane (D1861, Invitrogen, Carlsbad, USA) in sodium borate buffer (pH 8.5). NHS-PEG-Mal was then applied to the cantilever, which was then washed in ddH<sub>2</sub>O. Subsequently C11L34 antibodies at a concentration of 2.5 mg/ml were bound to the pegylated cantilevers at 8 °C for 2 h. The cantilever was finally washed with PBS.

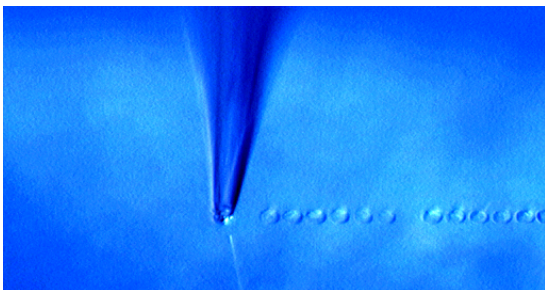
### **Preparation of cover glass surfaces**

Cover glass slips were sonicated in 50% (v/v) 2-propanol and ddH<sub>2</sub>O for 15 min and thoroughly rinsed with ddH<sub>2</sub>O. They were then oxidized in 50% (v/v) sulfuric acid and hydrogen peroxide (30%) for 45 min and were then again well rinsed with ddH<sub>2</sub>O. The oxidized cover glass slips were silanized with a mixture of 2% 3-aminopropyltrimethoxysilane, 90% EtOH, 8% ddH<sub>2</sub>O for 1 h. Cover glasses were thoroughly rinsed with pure EtOH first and ddH<sub>2</sub>O afterwards, and were baked at 80 °C for 30 min. After 30 min soaking in 50 mM sodium borate buffer, pH 8.5 the cover glasses were treated with 50 mM NHS-PEG-maleimide (MW 5000) in the sodium borate buffer for 1 h and then rinsed with ddH<sub>2</sub>O.

In case of the SMC&P experiments depot and target oligomers were reduced, purified and dissolved again. The reduced thiolated depot and target oligomers were deposited with a microplotter (GIX, Sonoplot, Middleton, USA), nonbound DNA was washed away with ddH<sub>2</sub>O. Transfer oligomers were deposited on top of the depot area. Nonbound transfer strands were washed away with 4xPBS buffer. (Details on the microstructuring process are given in the following section.) The sample was then covered with 50 mM sodium borate buffer, pH 8.5, 500 mM NaCl, 10 mM TCEP for 30 min for deprotonation of amines and quenching of unreacted maleimides. The sample was then rinsed with 50 mM sodium borate buffer, pH 8.5, 500 mM NaCl and incubated for 1h with 10 mM NHS-PEG-Mal dissolved in 50 mM sodium borate buffer, pH 8.5, 500 mM NaCl. It was washed with PBS, then reduced GCN4 peptides at a concentration of 100  $\mu$ M in 50 mM sodium phosphate buffer, pH 7.2, 250 mM NaCl, 10 mM EDTA were added for 1 h. The sample was rinsed again with PBS.

For single molecule force spectroscopy reduced thiolated depot or target oligomers or the reduced GCN4 peptide was bound to the pegylated cover glass slips and the sample was thoroughly rinsed with water.

### **Structuring surfaces with a Microplotter**



Due to the limited travel range of the AFM, the depot and target area have to be created in a distance of several micrometers. For this reason these areas are produced by microstructuring the cover glass with a microplotter (GIX, Sonoplot, Middleton, USA). A standard glass capillary (World Precision Instruments, Inc.) with an inner diameter of 30  $\mu$ m was used, which results in spots of the diameter of 45  $\mu$ m to 50  $\mu$ m on the cover glass

(dispenser voltage 3V and 0.1 s dispensing time). The prepared DNA Oligomer solutions (see previous section) were plotted on the pegylated cover glass in two 800  $\mu\text{m}$  long lines for depot and target, which were separated by a 20  $\mu\text{m}$  to 30  $\mu\text{m}$  broad gap.

After plotting the depot line, the cover glass was rinsed with 5 ml (4x PBS) directly in the sample holder without moving it. In a second step, the transfer strand was plotted onto the depot line. Operating experience showed that in the case of hybridizing DNA via Microplotter a contact time (capillary on the cover slide) of around 20 s per spot optimized the density of hybridized transfer strands. Afterwards the sample was rinsed as before. In a last step, the target strand was plotted in same manner as the depot.

### **Oligomer sequences**

thiolated depot oligomer

5' SH - TTT TTT CAT GCA AGT AGC TAT TCG AAC TAT AGC TTA AGG ACG TCA A

thiolated target oligomer

5' CAT GCA AGT AGC TAT TCG AAC TAT AGC TTA AGG ACG TCA ATT TTT - SH

transfer oligomer with amine and Atto647N

5' (Atto647N) - TTG ACG TCC TTA AGC TAT AGT TCG AAT AGC TAC TTG CAT GTT TTT TTT - NH<sub>2</sub>

thiolated transfer oligomer

5' TTG ACG TCC TTA AGC TAT AGT TCG AAT AGC TAC TTG CAT GTT TTT TTT - SH

1. H. Gump, S. W. Stahl, M. Strackharn, E. M. Puchner, H. E. Gaub, Ultrastable combined atomic force and total internal reflection fluorescence microscope [corrected]. *The Review of scientific instruments* **80**, 063704 (Jun, 2009).
2. E. Florin, Sensing specific molecular interactions with the atomic force microscope. *Biosensors and Bioelectronics* **10**, 895 (1995).
3. H. J. Butt, M. Jaschke, Calculation of thermal noise in atomic-force microscopy. *Nanotechnology* **6**, 1 (1995).

4. J. Morfill *et al.*, Affinity-matured recombinant antibody fragments analyzed by single-molecule force spectroscopy. *Biophys J* **93**, 3583 (Nov 15, 2007).
5. A. Krebber *et al.*, Reliable cloning of functional antibody variable domains from hybridomas and spleen cell repertoires employing a reengineered phage display system. *J Immunol Methods* **201**, 35 (Feb 14, 1997).
6. H. Bothmann, A. Pluckthun, Selection for a periplasmic factor improving phage display and functional periplasmic expression. *Nat Biotechnol* **16**, 376 (Apr, 1998).
7. J. Hanes, L. Jermutus, S. Weber-Bornhauser, H. R. Bosshard, A. Pluckthun, Ribosome display efficiently selects and evolves high-affinity antibodies in vitro from immune libraries. *Proc Natl Acad Sci U S A* **95**, 14130 (Nov 24, 1998).